UCRL- 92311 Rev. 1
PREPRINT

Gamma Radiation Effects on Corrosion, I. Electrochemical Mechanisms for the Aqueous Corrosion Processes of Austenitic Stainless Steels Relevant to Nuclear Waste Disposal in Tuff

Robert S. Glass
George E. Overturf
Richard A. Van Konynenburg
R. Daniel McCright

Corrosion Science

January 1986

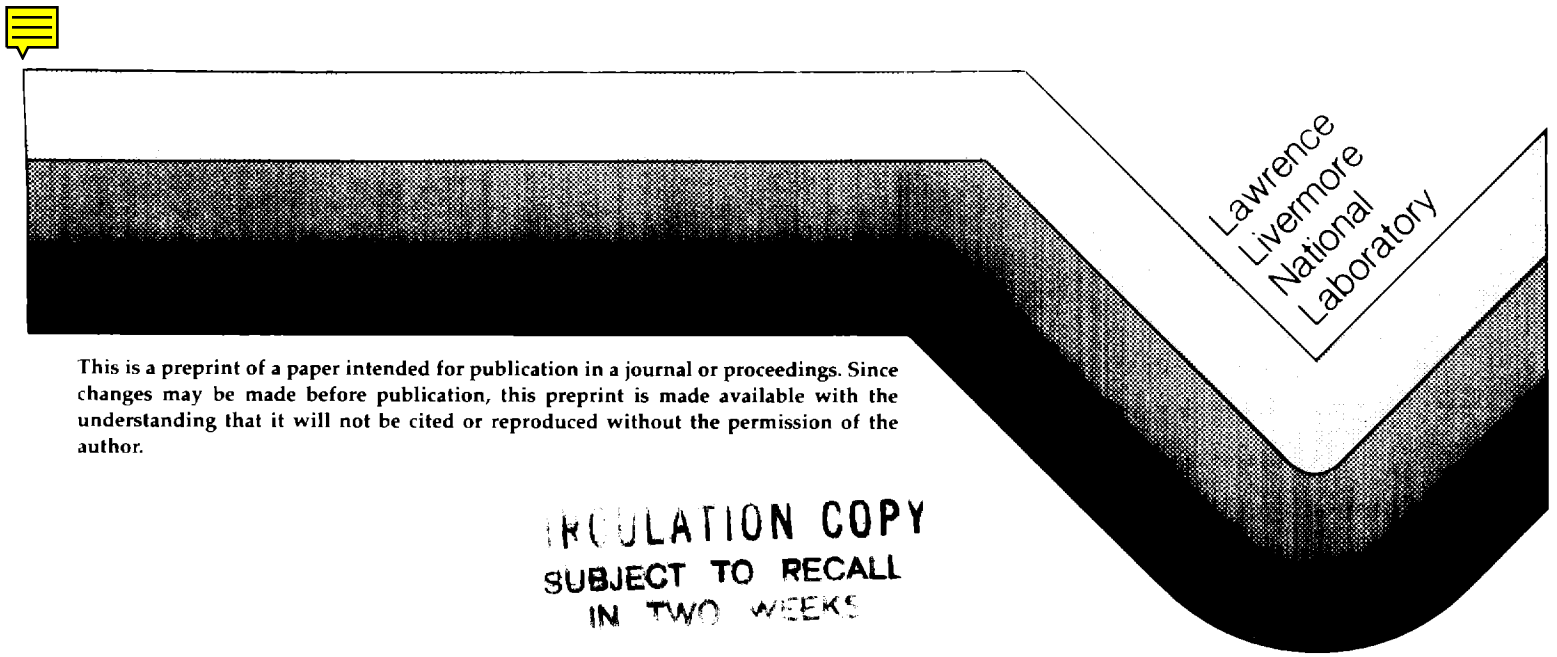

Gamma Radiation Effects on Corrosion, I. Electrochemical Mechanisms for the Aqueous Corrosion Processes of Austenitic Stainless Steels Relevant to Nuclear Waste Disposal in Tuff

Robert S. Glass, George E. Overturf,
Richard A. Van Konynenburg, and R. Daniel McCright

Lawrence Livermore National Laboratory
Livermore, CA 94550

Abstract

The effects of gamma irradiation on the corrosion mechanisms of 304L and 316L stainless steels in groundwater from a proposed nuclear waste repository site in tuffaceous rock are presented. When gamma irradiation is initiated, corrosion potential shifts in the positive direction are observed. These potential shifts are associated with the radiation-induced production of hydrogen peroxide. The electrochemical mechanisms involved in the corrosion potential shifts, as well as the subsequent effect on pitting resistance, are considered.

Introduction

The safe disposal of high level nuclear waste materials in geological media represents a current technological challenge. One aspect of this challenge is the development of barrier packages that must be environmentally stable for time periods of 300 to 1000 years. In designing metallic engineered barriers for waste disposal, the susceptibility to potential corrosion failure modes such as uniform corrosion, pitting, crevice attack, hydrogen embrittlement, and stress-corrosion cracking must be evaluated. In addition to these failure modes normally encountered in corrosion studies, the interaction of gamma radiation from the waste with the surrounding chemical environment must be understood in light of the possibility of effects on corrosion mechanisms.

---

*Work performed under the auspices of the U.S. Department of Energy by the Lawrence Livermore National Laboratory under contract number W-7405-ENG-48.

The interaction of gamma radiation with aqueous solutions produces a host of transient radicals, ions, and stable molecular species including H•, •OH, e^-_{aq}, H_3O^+, OH^-, H_2, H_2O_2, O_2, O_2^-, and HO_2.[1-3] Species such as e^-_{aq}, H•, and H_2 can act as reducing agents, while others such as H_2O_2, •OH, O_2, O_2^- and HO_2 can act as oxidizing agents. As a result of the production of such species under gamma irradiation, there may be alterations in the rates or mechanisms of corrosion attack modes.

Previous investigations have found an increased susceptibility of sensitized 304 stainless steel towards intergranular stress corrosion cracking in high temperature water under gamma irradiation.[4,5] Other reports have claimed an increased resistance to crevice corrosion for austenitic stainless steels in aqueous solutions under gamma irradiation.[6] For carbon steel and 304 stainless steel, gamma irradiation in high temperature (250°C) water containing low oxygen levels has been shown to increase the release rates of insoluble corrosion products but not to increase the release rates of soluble products.[7]

Several reports have demonstrated or discussed effects of gamma irradiation on the corrosion potentials of austenitic stainless steels in aqueous media.[6, 8-12] Much of this work has been performed in acidic or single component media where still a complicated corrosion potential behavior is observed that reflects a balance between the reducing and oxidizing species generated under radiolysis for the particular experimental conditions used (e.g., aeration vs. deaeration). Shifts of the corrosion potential in the positive direction have generally been observed under gamma irradiation of oxygenated aqueous systems.

In general, a fundamental understanding of the effect of gamma irradiation on the mechanisms of corrosion of austenitic stainless steels is lacking. In particular, in near-neutral aqueous environments the introduction of new electrochemical reactions by the radiolytically-generated oxidants has received little mechanistic investigation. However, species such as H_2O_2, O_2, HO_2, O_2^-, etc., which are generated radiolytically, are generally assumed to increase the oxidizing nature of the environment.

The effects of gamma irradiation on waste package corrosion mechanisms in environments relevant to proposed nuclear waste repository sites are just beginning to be explored. One site under current consideration for a potential nuclear waste repository is located in Yucca Mountain adjacent to the Nevada Test Site. Although the repository horizon at this site would be in densely welded tuff above the static water table, intrusions of water could occur from matrix flow through the rock or episodically through fractures in the rock. The low annual precipitation at the site and low rate of percolation of this water downward minimizes the anticipated amount of water entering the waste package environment. For this repository location, austenitic stainless steels (e.g., 304L, 316L) have been proposed for use as waste container materials.[13,14]

In addition to groundwater containing naturally occurring concentrations of dissolved species, it is also of interest to consider solutions in which these species are more concentrated. Evaporative processes at the repository site could lead to concentration of the electrolyte since groundwater may intrude into the repository site prior to the time that the container surface has cooled to below boiling temperature and then evaporate and leave behind salt deposits. Subsequent repetition of these events at the same locations could conceivably result in local salt build-up. When the container surface temperature has cooled to below the boiling point, further wetting at locations of salt build-up could lead to a concentrated electrolyte. This concentrated electrolyte could only result from a sequence of low probability events. However, observing the performance of candidate container materials under such concentrated solute conditions is instructive and is also necessary for selection of a material that will meet regulatory requirements for long-term integrity of the container.

In this paper, initial results are reported on the in-situ electrochemical characterization of the response of 304L and 316L to gamma-irradiated groundwater that is regional to the potential tuff repository site. Corrosion potential measurements and anodic polarization curves were obtained under gamma irradiation. The major specie responsible for the observed electrochemical changes is shown to be radiolytically-generated H_2O_2. Initial assessment of the effect of radiolysis on corrosion parameters (e.g., pitting resistance) of

316L is given. The electrochemical mechanisms leading to the observed corrosion potential behavior under gamma irradiation are explored. Despite the fact that this study was site-specific, the principal mechanisms and the general results should be applicable to any near-neutral (or somewhat alkaline) aqueous system with low concentrations of solute species.

Experimental

Austenitic stainless steels AISI 304L and 316L were used in the solution annealed condition. The compositions of the alloys used are given in Table 1. Rods of these materials 0.318 cm in diameter were used as working electrodes. All samples were polished with 600 grit SiC paper, followed by 5μ, 1μ, 0.3μ and 0.05μ Al_2O_3 slurries prior to use.

The groundwater used in these experiments was obtained from well J-13, which is located near the repository site. The J-13 well penetrates the water table at a lower elevation than that of the potential repository. Water from this well has percolated through the densely welded tuff layer characteristic of the region. The composition of the groundwater is shown in Table 2.[15] In some experiments, concentrated forms of this groundwater (e.g., 10x and 100x) were used. Concentration by 100x is above what is considered likely in the repository, but was used to bound the possible conditions. Boil-down under atmospheric pressure was used to obtain the more concentrated electrolytes. When additions of other species were made, analytical reagent chemicals (H_2O_2 and NaCl) or ultra-high purity gases (H_2 and Ar) were used. Unless otherwise indicated all experiments were performed in initially air-saturated solutions vented to the atmosphere.

A diagram of the electrochemical apparatus used in this work is shown in Fig. 1. The reference electrode (SCE) is placed in a reservoir containing saturated KCl in the upper chamber. The upper and lower chambers are connected by a Luggin probe, approximately 1.4 m long, filled with saturated KCl. The lower chamber, which is the only part of the system surrounded by the gamma sources, contains the Pyrex electrochemical cell. The cell itself has inlets for the reference electrode Luggin probe, the working electrode, and a coiled Pt-wire counter electrode, and a port for deaeration. In this arrangement the reference electrode is isolated from the gamma sources.

The gamma sources consisted of ^{60}Co pencils oriented vertically in a cylindrical array. The lower chamber of the electrochemical cell was inserted into this array, at the center of which the dose rate was 3.3 Mrad/hr (±20%). All experiments were performed at 30°C (±5°C).

Corrosion potential vs. time and potentiodynamic anodic polarization curves were obtained with the aid of a Princeton Applied Research Model 273 potentiostat and Model 351 microprocessor-controller. All polarization curves began at approximately 200 mV cathodic to the corrosion potential and proceeded in the anodic direction at a scan rate of 0.166 mV/s.

Results and Discussion:

Aqueous Environment and Radiation Chemistry:

As noted above, Table 2 represents the composition of groundwater which is regional to the proposed repository site. The low concentrations of solute species, particularly the detrimental anion Cl^-, and the near-neutral pH (7.6) suggest that this electrolyte should be relatively benign with regard to corrosion of austenitic stainless steels.

Before proceeding to interpret the electrochemical experiments, it is helpful to consider what is known about bulk radiation chemistry of aqueous solutions from past work in this field. Because the groundwater contains only low concentrations of solutes, its bulk radiation chemistry should be very similar to that of pure water. In the case of pure, deaerated water the primary radiolytic species under gamma irradiation are $H^\bullet$, $^\bullet OH$, e^-_{aq}, H_3O^+, OH^-, H_2, H_2O_2, and HO_2.[3] In an inert, closed vessel these species undergo reactions with each other to reform water, resulting in small steady-state concentrations of radicals and molecular species and no further decomposition of water. The species having the highest concentrations are H_2 and H_2O_2.[16]

If the water contains a few ppm of dissolved oxygen, the reducing species $H^\bullet$ and e^-_{aq} are rapidly converted to HO_2 and O_2^-, respectively. If the pH is much greater than about 4.9, the HO_2 ionizes to form additional O_2^-.[17] In the case of oxygenated water, H_2 and $H^\bullet$ are suppressed, and the most abundant

species are O_2 and H_2O_2.[16] At the proposed repository site, the J-13 well water would be in equilibrium with air and would therefore contain several ppm of O_2.[13,14,18]

The pH region from 7 to 10 is of the most interest for J-13 well water. With evaporation and concentration of this electrolyte (i.e., to 100x concentration), calcium silicate and carbonate precipitate, and the pH rises to around 10. The geochemistry of J-13 well water has been discussed previously.[18] The yields (G-values) of the primary species in the radiolysis of pure water are nearly independent of pH in the region from pH 4 to 10.[3] Under radiolysis of J-13 well water we can therefore expect an oxidizing environment with O_2 and H_2O_2 as the dominant species, a smaller concentration of O_2^-, and much smaller steady-state concentrations of H_2, $^{\bullet}OH$, and $H^{\bullet}$. It should be noted that we do not expect significant production of nitric acid in these experiments because of the small air volume and the short duration of the experiments. Nitric acid has been shown to form from irradiation of air in contact with aqueous solutions, rather than from dissolved N_2 in the solutions themselves. In the experiments reported here we would expect a maximum HNO_3 production of approximately 8×10^{-6} M. A calculation, based upon the results of Burns et. al.,[19] is given in Appendix I. The additional amount of NO_3^- would thus be small compared to the amount already present in J13 water (1.5×10^{-4} M), and the additional H^+ would easily be buffered by the HCO_3^- (2×10^{-3} M). Under repository conditions, HNO_3 production may be more important, because of the higher radiation doses and higher gas-to-liquid volume ratios. The effects of the radiolytic species on electrochemical mechanisms will be outlined in the following discussion.

Electrochemical Potential Measurements

The corrosion potential of austenitic steels is significantly affected by gamma irradiation due to the generation of new oxidizing species. Upon imposition of the gamma field, the corrosion potential of both 304L and 316L in a series of electrolytes related to J-13 well water shifted in the positive direction, typically by 150-250 mV. Typical behavior for 316L in 100x concentrated J-13 water (pH 10.3) is shown in Fig. 2. In this and in succeeding figures, "on" refers to lowering of the cell into the center of the gamma

sources and "off" refers to raising the cell 1.3 to 1.5 m above the sources where the cell would be shielded by intervening water. Two "on/off" cycles are shown. Similar positive potential shifts upon imposition of the gamma field were observed for 316L in non-concentrated J-13 well water (pH 7.6) and when 304L was the electrode material.

These experiments indicated that the positive shifts in the corrosion potential resulted from the more oxidizing environment produced by gamma irradiation. Such potential shifts may be generic to austenitic stainless steels, since the same behavior was observed with both 304L and 316L in J-13 well water and its more concentrated forms. As will be discussed more fully below, the initial rapid rise of potential upon imposition of the gamma field is likely the result of the generation of H_2O_2 and $\cdot OH$ radicals in the solution layers next to the electrode surface. The subsequent slower rise of potential with time corresponds in part to the slower buildup of the steady-state bulk concentration of H_2O_2.

Following exposure of 316L stainless steel to gamma-irradiated environments, the electrochemical cell was removed from the gamma sources and the corrosion potential was continuously monitored for several hours (generally more than 14 hours). The potential in each case was found to remain in the range of the high (relative) positive values that were observed immediately after termination of the irradiation.

In order to test whether the observed effects resulted from stable oxidizing species in the solution, permanent changes in the oxide film on the electrode, or both, the following experiment was performed: Following an "on/off" cycle for 316L stainless steel in J-13 water, the cell was removed from the gamma facility and the irradiated solution was replaced by "fresh" non-irradiated J-13 water. When this was done, the corrosion potential immediately shifted in the negative direction as shown in Fig. 3 (larger negative potential shifts than that shown for the experiment in Fig. 3 were also frequently observed). This data, in conjunction with the rapid rise of the potential upon initiation of irradiation, appear to indicate that the positive potential shifts observed are due mostly to radiolytically generated stable oxidizing species acting as cathodic depolarizers. Structural modifica-

tion of the oxide film, as reflected in corrosion potential changes, would be expected to show a longer time dependence. However, it is also evident that some long-term changes in the oxide film are probably produced since the corrosion potential does not appear to return to the pre-radiolysis potential (apparent extrapolated steady-state value) when the fresh solution is introduced. The oxide film alterations are produced through the action of the radiolytic oxidants on the film. Structural modifications of the oxide film may be confined to the outer layers.

As discussed above, H_2O_2 is the dominant stable oxidizing species produced under radiolysis. In J-13 well water, following 3.5 hours of exposure at the dose rate employed in this study, the concentration of H_2O_2 produced was measured to be 0.14 mM using the titanium oxalate method.[20] To see whether H_2O_2 alone could produce the potential shifts of the magnitude observed under irradiation, H_2O_2 was added to the fresh J-13 water in the cell from the experiment above, producing a concentration of about 0.4 mM. The potential was observed to shift in the positive direction immediately (see Fig. 3). Positive potential shifts similar in magnitude to this were also observed when H_2O_2 was added to J-13 solution in which an unirradiated 316L electrode was immersed. The observed change when H_2O_2 was added to the solution, coupled with the knowledge that H_2O_2 is the most concentrated radiolytic species present in an irradiated, aerated solution, provides strong evidence that it is responsible for the long-term potential shift observed upon irradiation in these solutions. However, the production of other oxidizing species (e.g., transient $\cdot OH$ radicals) under radiolysis will also assist in producing positive potential shifts.

To shed further light on the electrochemical effects of irradiation, and to separate possible electrode effects from solution effects, some experiments were performed using smooth platinum as the working electrode. In contrast to the behavior observed for austenitic stainless steels under irradiation, smooth Pt in J-13 well water shows different behavior, as shown in Fig. 4. Upon initiation of irradiation the open-circuit potential immediately drops to more negative values.

The results for platinum can be understood as follows: Pt, as an electrode, is very responsive to the presence of $H^\bullet$ and H_2, which are also

produced in radiolysis. In the bulk of the solution, H• is expected to react rapidly with O_2, as stated above, and to have a very low steady-state concentration. However, near the electrode surface, it should be available for interfacial electrochemical reactions. Likewise H_2, though present at small concentration in the bulk and normally not very reactive in aqueous solutions at room temperature, can be an important factor at the surface of a Pt electrode, which is catalytic to H_2. The open-circuit potential for Pt is therefore determined by the hydrogen reaction as well as by mechanisms involving H_2O_2. It can be expected to be particularly responsive to the very small concentrations of H• and H_2. When irradiation is terminated, the potential rapidly rises as H_2 at the surface is swept away (by diffusion or reaction) and Pt rapidly responds to the presence of a larger concentration of H_2O_2. Since the steady-state H_2 concentration in an irradiated, oxygenated solution is much smaller than that of H_2O_2, the H_2 could thus be depleted easily, leaving considerable H_2O_2 in the solution to affect the potential. This would shift the open-circuit potential in the positive direction. The cathodic spikes observed in the "on/off" cycles are not completely understood; however, they could indicate a greater transient concentration of H• and/or H_2 at the electrode surface. It is to be noted that the open-circuit potential for Pt in this media will also be influenced by solute species other than H_2 and H_2O_2 (e.g., NO_3^-).

Previous investigations have shown decreased levels of H_2O_2 produced under gamma irradiation when inert gases were used to purge the system during radiolysis.[21,22] This results from the removal of O_2 from the system, which frees the reducing radicals (H• and e^-_{aq}) to attack the H_2O_2. In another experiment using Pt as the sensing electrode in J-13 water, the solution was purged with argon before and during irradiation. In this case, the open-circuit potential under irradiation was much more negative (attaining a value of approximately -330 mV) than that corresponding to the air-saturated experiment shown in Fig. 4. This indicates an enhanced response to the reducing species H• and H_2 when formation of the oxidizing species H_2O_2 is inhibited.

The response of a 316L electrode in J-13 water to which both H_2O_2 and H_2 were added sequentially is shown in Fig. 5. When two drops of 30% H_2O_2 solution were added, producing a concentration of approximately 1.0 mM, the corrosion potential immediately shifted positively. Upon subsequently purging the

solution with H_2, however, 316L showed no response. This indicates that the 316L electrode, with an oxide film formed under the present conditions, acts as a poor "hydrogen" electrode. It is believed to have a low rate constant for dissociation of H_2 on its surface. In addition, the removal of O_2 from solution by purging with H_2 is observed to have no effect, on the timescale of our experiment. However, the response of this material to H_2O_2 is dramatic. Although, on this experimental timescale the corrosion potential of 316L is not significantly affected by molecular H_2 when H_2O_2 is also present, the response to radiolytically-generated atomic hydrogen produced in the solution layers immediately adjacent to the electrode surface has not been determined.

Electrochemical Mechanisms:

A large number of electrochemical reactions involving oxidizing species are possible in gamma-irradiated aqueous solutions. Of course, the corrosion potential will be a mixed potential resulting from the superposition of the kinetics of all the anodic and cathodic reactions occurring on the surface. The situation is so complex that the relative contributions of reactions of secondary importance are difficult to ascertain. The relative importance of the redox reactions will depend upon such factors as dose rate, pH, relative concentrations, electron transfer rate constants, temperature, relative concentrations of "scavenger" species, etc.

In considering the electrochemical behavior of Pt in non-irradiated, high-purity aqueous solutions of H_2O_2, Bockris and Oldfield[23] proposed the following reaction as determining the open-circuit potentials observed:

$$(^{\bullet}OH)_{ads} + e^- \rightleftarrows OH^- \qquad (1)$$

In this equation, adsorbed hydroxyl radicals on the Pt surface participate in an electrochemical equilibrium with hydroxide ions in solution. The adsorbed hydroxyls originate from a surface-catalyzed decomposition of H_2O_2, i.e.,

$$H_2O_2 \xrightarrow{Pt} 2(^{\bullet}OH)_{ads} \qquad (2)$$

In their work, the pH dependence of the open-circuit potential of Pt was given as

$$E_{oc,Pt} = 0.594 - 0.059\ pH \quad \text{volts vs. SCE.} \tag{3}$$

The potential was found to be independent of the concentration of H_2O_2 down to 10^{-6} M. At concentrations above this value, a saturation surface coverage of hydroxyl radicals was postulated. At a pH of 7, the E_{oc} value for Pt would therefore be 0.181 V vs. SCE. At incomplete surface coverages, more negative potentials were observed. Since their work was performed in high-purity aqueous solutions of H_2O_2, one would not necessarily expect the same potential dependence in irradiated J-13 well water, which in addition to H_2O_2 contains ppm levels of such other solute species such as NO_3^-, SO_4^{-2}, HCO_3^-, Cl^- etc., as well as other radiolytic species which may also influence interfacial processes.

Subsequent to this work, Gerischer and Gerischer[24] proposed a more complicated scheme to explain the electrochemical behavior of Pt in aqueous solutions of H_2O_2. In their scheme, H_2O_2 was conceived to be electrochemically discharged on Pt into either adsorbed hydroxyl or perhydroxyl (HO_2) radicals in cathodic or anodic reactions, respectively. With a relative importance depending upon pH, the adsorbed hydroxyls could then participate in a cathodic process to liberate OH^-, whereas the adsorbed HO_2 species could liberate O_2 by an anodic process. In addition, and concurrently, these adsorbed species, $\cdot OH$ and HO_2, could participate in a cyclical catalytic mechanism to decompose H_2O_2 on the surface, liberate H_2O and O_2, and regenerate the original adsorbed species ($\cdot OH$ and HO_2). This catalytic scheme would be more important at higher pH. The balance of anodic and cathodic reactions in this cyclical catalytic scheme would then determine the open-circuit potential for Pt.

In the case of gamma radiolysis, where both $\cdot OH$ and H_2O_2 are generated in solution and may directly adsorb or decompose on the surface, respectively, either of the above mechanisms could be important in helping to determine the corrosion potential of austenitic stainless steels. In the solution layers next to the electrode, both species would be important in this regard. In the bulk, only the generation of H_2O_2 would be important as the $\cdot OH$ radicals have

too short a lifetime to diffuse appreciably.[2,3,16] As stated previously, the generation of both H_2O_2 and •OH in the solution layers next to the electrode are important for the initial rapid rise in potential observed upon imposition of the gamma field. The subsequent slower rise of potential is probably due to the bulk generation of H_2O_2 and its diffusion to the electrode surface. If the Gerischer mechanism for H_2O_2 decomposition can be applied to the behavior of austenitic steels in aqueous solution under irradiation, another oxidizing species, O_2, would also be present at the electrode surface and available to participate in electrochemical reactions.

Although reactions such as (1) and (2), or, alternatively, the catalytic mechanism of Gerischer and Gerischer, may be very important in determining the corrosion potential of austenitic stainless steels in aqueous solution under gamma radiolysis, the situation is complex in that other reactions (e.g., metal dissolution) also play a role. Stainless steel forms a much more complex electrochemical interface with aqueous solutions than does Pt and may not have a surface saturation coverage of adsorbed hydroxyl species. A lower rate constant for the decomposition of H_2O_2, or other reactions with the oxide film, may account for this. In any case, theory would not a-priori predict the same open-circuit potential behavior for austenitic stainless steels under gamma irradiation as is observed for Pt in non-irradiated, high-purity aqueous solutions of H_2O_2. The mechanisms leading to the positive corrosion potential shifts for austenitic stainless steel under gamma irradiation, although clearly associated with the production of H_2O_2, need further clarification.

The anodic and cathodic reactions that are believed to be of major importance in determining the corrosion potentials of austenitic stainless steels under gamma irradiation are listed below. Based upon the results presented above, we believe that these reactions will probably predominate under gamma irradiation in aerated aqueous systems similar to those of J-13 well water and its concentrated (10x, 100x) forms when the pH is neutral to mildly alkaline.

Cathodic reactions:

$$(\bullet OH)_{ads} + e^- \rightleftarrows OH^- \qquad (4)$$

$$O_2 + 2H_2O + 4e^- \rightarrow 4OH^- \quad (5)$$

$$O_2^- + H_2O + e^- \rightarrow HO_2^- + OH^- \quad (6)$$

(small contribution)

$$HO_2^- + H_2O + 2e^- \rightarrow 3OH^- \quad (7)$$

(very small contribution)

Anodic reactions:

$$Fe \rightarrow Fe^{+2} + 2e^- \quad (8)$$

$$Cr \rightarrow Cr^{+3} + 3e^- \quad (9)$$

$$Ni \rightarrow Ni^{+2} + 2e^- \quad (10)$$

The coupling of the cathodic processes with metal dissolution reactions will result in the observed mixed corrosion potential. Again, the equilibrium described in equation (1) could be replaced by the cyclical catalytic mechanism for H_2O_2 decomposition proposed by Gerischer and Gerischer.[24]

Localized Corrosion Effects

For practical applications, it is important to know what the effect of the positive corrosion potential shifts will be on the corrosion mechanism(s). In particular, it would be useful to find out whether the positive potential shifts increase the susceptibility of the material to pitting.

Initial results appear to indicate that the pitting susceptibility of 316L may be increased under gamma irradiation. This is shown by comparison of the anodic polarization curves in Fig. 6 obtained both in-situ in the gamma field and in unirradiated solution. The solution used in this case was 0.018M NaCl (650 ppm Cl^-) in deionized water. This solution represents a 100-fold increase in concentration of this particularly detrimental anion with respect to J-13 well water, and should be more conducive to pitting. Both scans began at 0.2 V cathodic to the corrosion potential.

For the non-irradiated case, the corrosion potential was -0.105 V vs. SCE. Upon scanning anodically, the pitting potential was found to be 0.324 V, as identified by the intersection of the extrapolated lines from the passive and pitting regions of the curve. The value of $E_p - E_{corr}$ is therefore 0.429 V. For the gamma irradiated case, the corresponding values for E_{corr} and E_p are 0.116 V and 0.313 V, respectively. This represents a separation of $E_p - E_{corr}$ of 0.197 V. Upon attaining the anodic limit, both scans shown in Fig. 6 were reversed to more cathodic potentials (these are not shown for clarity). Both curves showed hysteresis loops on these reverse scans characteristic of pitting, and the specimens were visibly pitted upon examination following completion of the cyclic polarizations.

The difference in pitting potentials observed ex-situ and under irradiation (11 mV) is not significant given the experimental method employed. Therefore, as determined from the potentiodynamic polarization technique, gamma irradiation appears to affect only the corrosion potential (shifting it in the positive direction) and leaves the pitting potential unchanged. If the difference, $E_p - E_{corr}$, is used as a measure of susceptibility to pitting, then the smaller values observed under irradiation would indicate decreased resistance. However, as E_p is still some 0.2 V more positive than E_{corr}, pitting would not be spontaneous under irradiation. Results similar to those in 0.018M NaCl solution (positive corrosion potential shift and no change in pitting potential under irradiation) were also obtained 0.1 M NaCl solution. Additional work is needed and is underway to evaluate the localized corrosion behavior (both pitting and crevice corrosion) of austenitic steels under gamma irradiation.

Conclusions

The conclusions from this study are as follows:

1. Gamma irradiation increases the oxidizing nature of the aqueous solutions used in this study through production of H_2O_2 and $\cdot OH$. These species account for the observed positive corrosion potential shift for 304L and 316L stainless steels. The corrosion potential shift is typically 150-250 mV, dependent upon the media, electrode material, and surface condition, and may be generic for

austenitic stainless steels in J-13 well water and in related (more concentrated) environments. Part of the shift is reversible by replacing the irradiated solution with fresh solution (i.e., is due to redox processes), and a smaller part appears to result from longer-term changes in the outer oxide layer.

2. By analogy to previous work on Pt in aqueous high-purity H_2O_2 media, the electrochemical equilibrium between adsorbed hydroxyl species and hydroxide ions in solution may be important in determining in part the corrosion potentials of stainless steel in irradiated aqueous solutions. Alternatively, a cyclical catalytic scheme for the decomposition of H_2O_2 involving adsorbed species (e.g., $\cdot OH$, HO_2, or O_2^-) participating in anodic and cathodic processes may also be important. However, a stainless steel surface certainly forms a more complex electrochemical interface than does a Pt surface, and other reactions also serve to establish a mixed corrosion potential, as discussed in the text.

3. The corrosion potential of 316L stainless steel does not appear to be sensitive to the presence of H_2 under the present experimental conditions (H_2O_2 also present) and time scales. While the corrosion potential is not sensitive to molecular H_2, it may be sensitive to atomic hydrogen, which is also produced under radiolysis. Molecular hydrogen may only play a role in helping to establish steady-state bulk H_2O_2 concentrations.

4. Results from potentiodynamic anodic polarization curves indicate that for 316L stainless steel in chloride media, the pitting potentials are essentially unchanged by gamma irradiation. As a result of the more positive corrosion potential under irradiation, the value of $E_p - E_{corr}$ decreases substantially with respect to the value obtained without irradiation. Therefore, the pitting resistance may be said to be decreased. However, in 0.018M NaCl solution at 30°C the shift of the corrosion potential of 316L stainless steel is not sufficient to shift it into the pitting regime.

References

1. C. J. Hochanadel, J. Phys. Chem. 56, 587 (1952).

2. A. O. Allen, "The Radiation Chemistry of Water and Aqueous Solutions," D. Van Nostrand and Co., Inc., Princeton, N.J., 1961.

3. J. W. T. Spinks and R. J. Woods, "An Introduction to Radiation Chemistry, 2nd edition", John Wiley and Sons, New York, 1976.

4. N. Fujita, M. Akiyama, and T. Tamura, Corrosion 37 335 (1981).

5. T. Furuya, T. Fukuzuka, K. Fujiwara, and H. Tomari, Kobe Res. Dev. 33, 43 (1983).

6. A. V. Byalobzheskii, "Radiation Corrosion", Israel Program for Scientific Translations, Jerusalem, 1970.

7. K. Ishigure, N. Fujita, T. Tamura, and K. Oshima, Nuclear Technology 50, 169 (1980).

8. G. H. Cartledge, Nature 186, 370 (1960).

9. S. Uchida, E. Ibe, and R. Katsura, Rad. Phys. Chem. 22, 515 (1983).

10. W. E. Clark, J. Electrochem. Soc. 105, 483 (1958).

11. W. G. Burns, W. R. Marsh, and W. S. Walters, Radiat. Phys. Chem. 21, 259 (1983).

12. J. J. Stobbs and A. J. Swallow, Met. Rev. 7, 95 (1962).

13. R. D. McCright, H. Weiss, M. C. Juhas, and R. W. Logan, Lawrence Livermore National Laboratory Report UCRL-89988, 1983.

14. J. N. Hockman and W. C. O'Neal, Lawrence Livermore National Laboratory Report UCRL-89820 Rev. 1, February 1984.

15. J. M. Delany, Lawrence Livermore National Laboratory Report UCRL-53631, March, 1985.

16. W. G. Burns and P. B. Moore, Rad. Effects 30, 233 (1976).

17. B. H. J. Bielski and J. M. Gebicki, "Species in Irradiated Oxygenated Water," Advances in Radiation Chemistry, Vol. 2, M. Burton and J. L. Magee, eds., Wiley-Interscience, New York, p. 177 (1970).

18. V. M. Oversby, Lawrence Livermore National Laboratory Report UCRL-53552, May 1984.

19. W. G. Burns, A. E. Hughes, J. A. C. Marples, R. S. Nelson, and A. M. Stoneham, Nature 295, 130 (1982).

20. R. M. Sellers, Analyst 105, 950 (1980).

21. C. J. Hochanadel in "Proc. U.N. Intern. Conf. Peaceful Uses At. Energy", Geneva, 1955, 7, 521, United Nations, Geneva (1955).

22. S. Gordon and E. J. Hart in "Proc. U.N. Intern. Conf. Peaceful Uses At. Energy, 2nd," Geneva, 1958, 29, 13, United Nations, Geneva (1958).

23. J. O'M. Bockris and L. F. Oldfield, Trans. Faraday Soc. 51, 249 (1955).

24. R. Gerischer and H. Gerischer, Z. Phys. Chem. 6, 178 (1956).

APPENDIX I.

Burns et al. have developed the following equation to quantify the production of nitric acid in a sealed air/water system.[18] As a first approximation we can apply this equation to our experiments, even though our system was open.

$$N = 2C_oR\,[1 - \exp\,(-1.45 \times 10^{-5}\ GDT)]$$

In this equation, N is the concentration of HNO_3 in moles ℓ^{-1}, D is the dose rate in Mrad/h^{-1}, R is the ratio of the volume of air to the volume of liquid, C_o is the concentration of nitrogen in air in moles ℓ^{-1}, t is the time of irradiation in hours, and the G value for the reaction is 1.9.

Substituting in the values for our experiments,

C_o = 0.032 mole ℓ^{-1}
R = 0.35
G = 1.9
D = 3.3 Mrad/h^{-1}
t = 4 h

yields a value for N of 8.1×10^{-6} moles ℓ^{-1}.

List of Tables

List of Figures

Fig. 1: Schematic of the electrochemical cell used in this work. Details are provided in the text.

Fig. 2: Corrosion potential behavior for 316L stainless steel in 100X concentrated J-13 well water under gamma irradiation. The solution was not exposed to irradiation prior to initiation of the first "on/off" irradiation cycle.

Fig. 3: Corrosion potential behavior for AISI 316L stainless steel in gamma-irradiated J-13 well water. Following the "off" half-cycle the irradiated solution was decanted and replaced by a fresh, unirradiated solution. Following this, H_2O_2 was added to solution at a concentration of 0.4 mM.

Fig. 4: Open-circuit potential behavior for platinum in gamma-irradiated J-13 well water.

Fig. 5: Response of the corrosion potential for 316L stainless steel in J-13 well water to successive additions of H_2O_2 and H_2. The points of introduction of these species into solution are indicated on the figure. In this experiment the addition of two drops of H_2O_2 (from a 30% solution) resulted in a solution concentration of approximately 1.0 mM. Purging of the solution with H_2 saturated the solution with H_2. The solution was continuously stirred with a magnetic stirrer in this experiment.

Fig. 6: Comparison of the potentiodynamic anodic polarization behavior for 316L stainless steel in 0.018 M NaCl solution in deionized water with and without gamma irradiation (—□—, unirradiated; ···○···, irradiated). The polarization curves were scanned anodically at a rate of 0.166 mV/s starting from approximately 200 mV cathodic of the corrosion potential in each case. In this figure, E_{corr} and E_p represent values of the corrosion potential and pitting potential, respectively, for the unirradiated case. The corresponding values for the irradiated experiment are indicated on the figure as $*E_{corr}$ and $*E_p$.

Table 1. Measured Analyses of the Electrode Materials

Alloy	Composition (wt%) C	Mn	P	S	Si	Ni	Cr	Mo	Co	Ti	Cu	Nb	N
304L	.022	1.55	.024	.025	.63	9.26	18.31	.36	.16	.002	.46	.01	.072
316L	.02	1.71	.033	.014	.56	10.29	16.51	2.07	.10	--	.28	--	.054

Table 2. Composition of J-13 Well Water

Species	Concentration (mg/l)
HCO_3^-	125
SO_4^{2-}	19
NO_3^-	9.6
Cl^-	6.9
F^-	2.2
Na^+	44
Ca^{2+}	12.5
K^+	5.1
Mg^{2+}	1.9
Si	27
pH = 7.6	

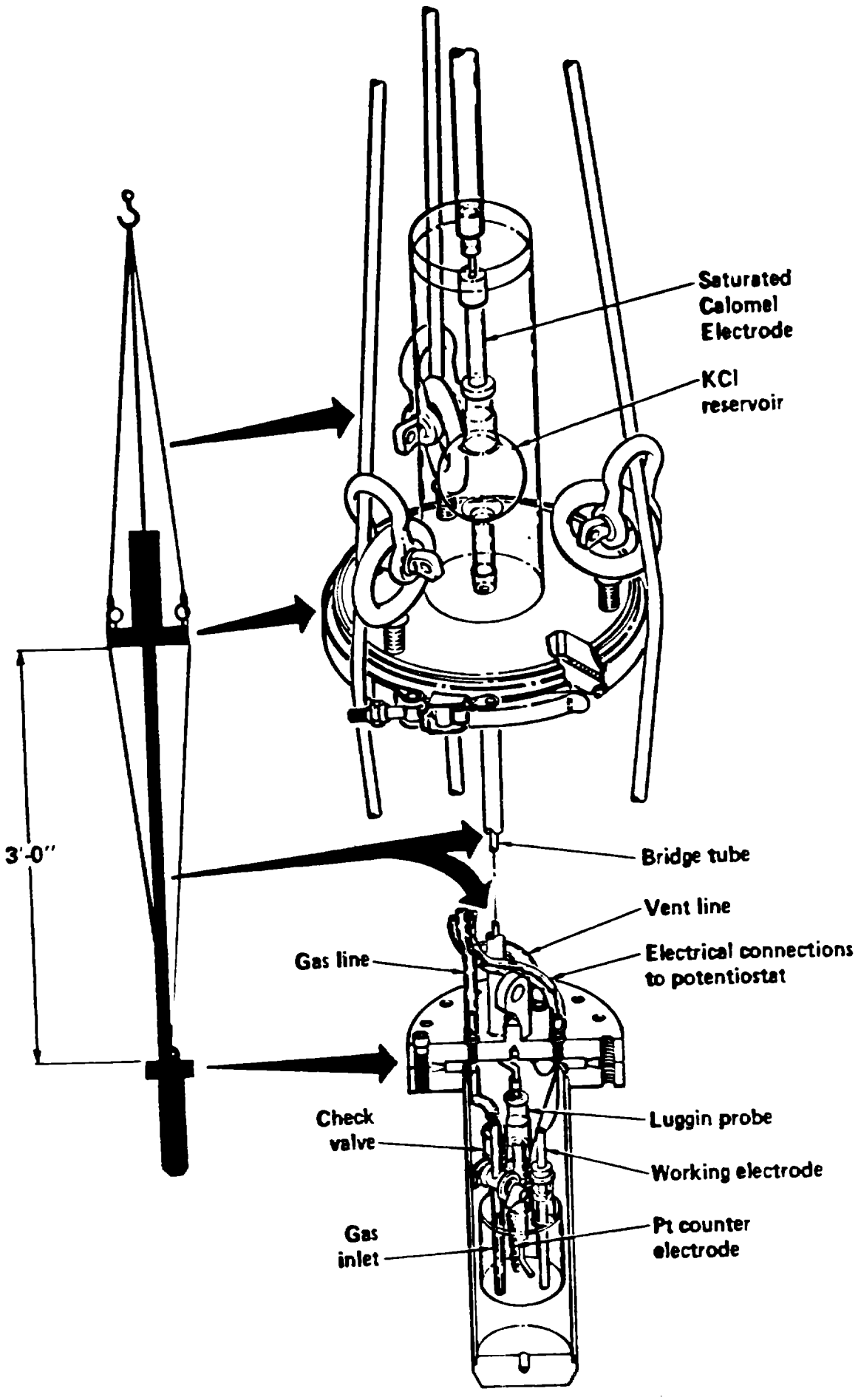
Saturated
Calomel
Electrode
KCl
reservoir
3'-0"
Bridge tube
Vent line
Gas line
Electrical connections
to potentiostat
Check
valve
Luggin probe
Working electrode
Gas
inlet
Pt counter
electrode

Figure 1

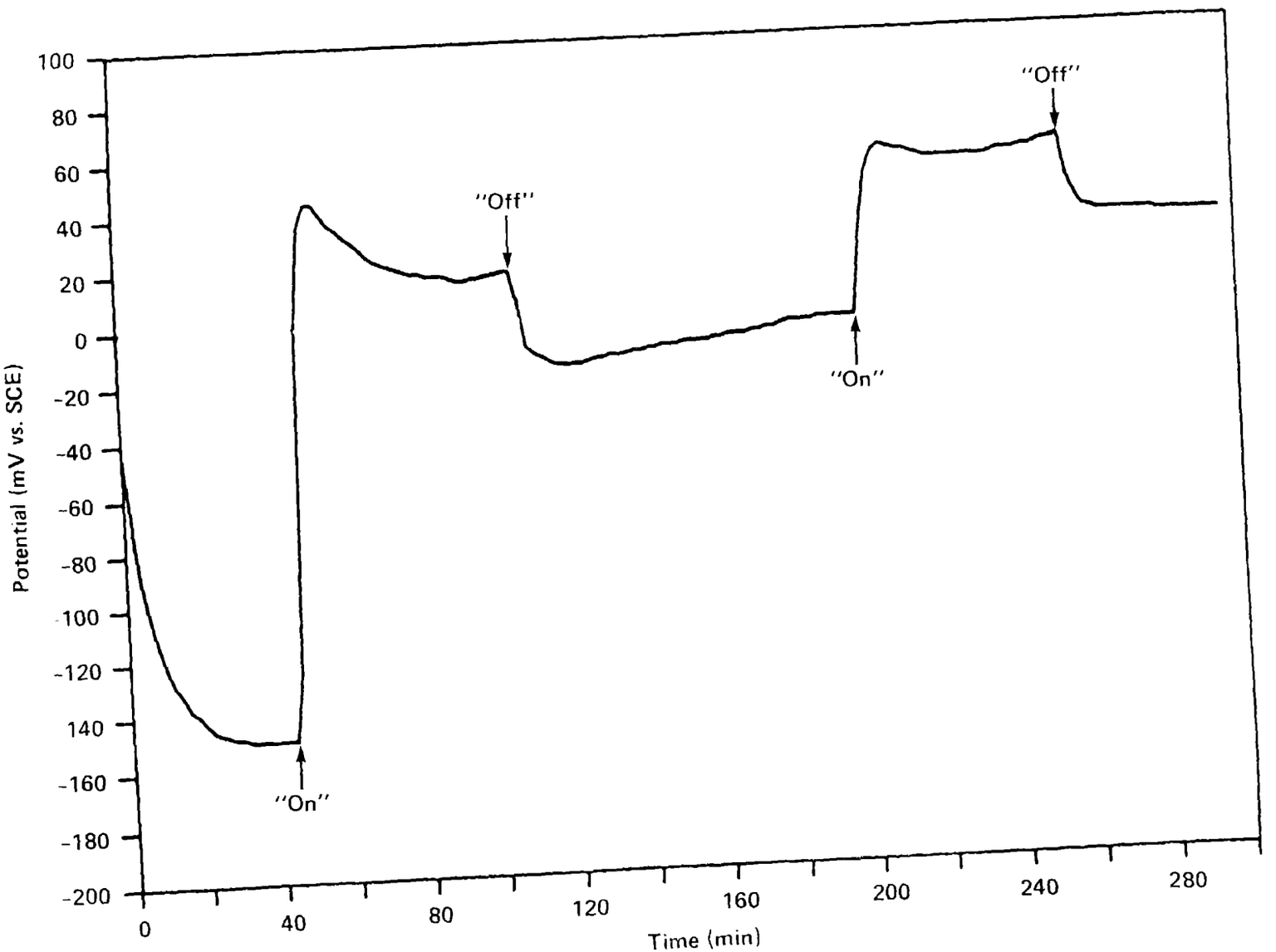
100
80
60
40
20
0
-20
-40
-60
-80
-100
-120
140
-160
-180
-200
Potential (mV vs. SCE)
"Off"
"Off"
"On"
"On"
0
40
80
120
160
200
240
280
Time (min)

FIGURE 2

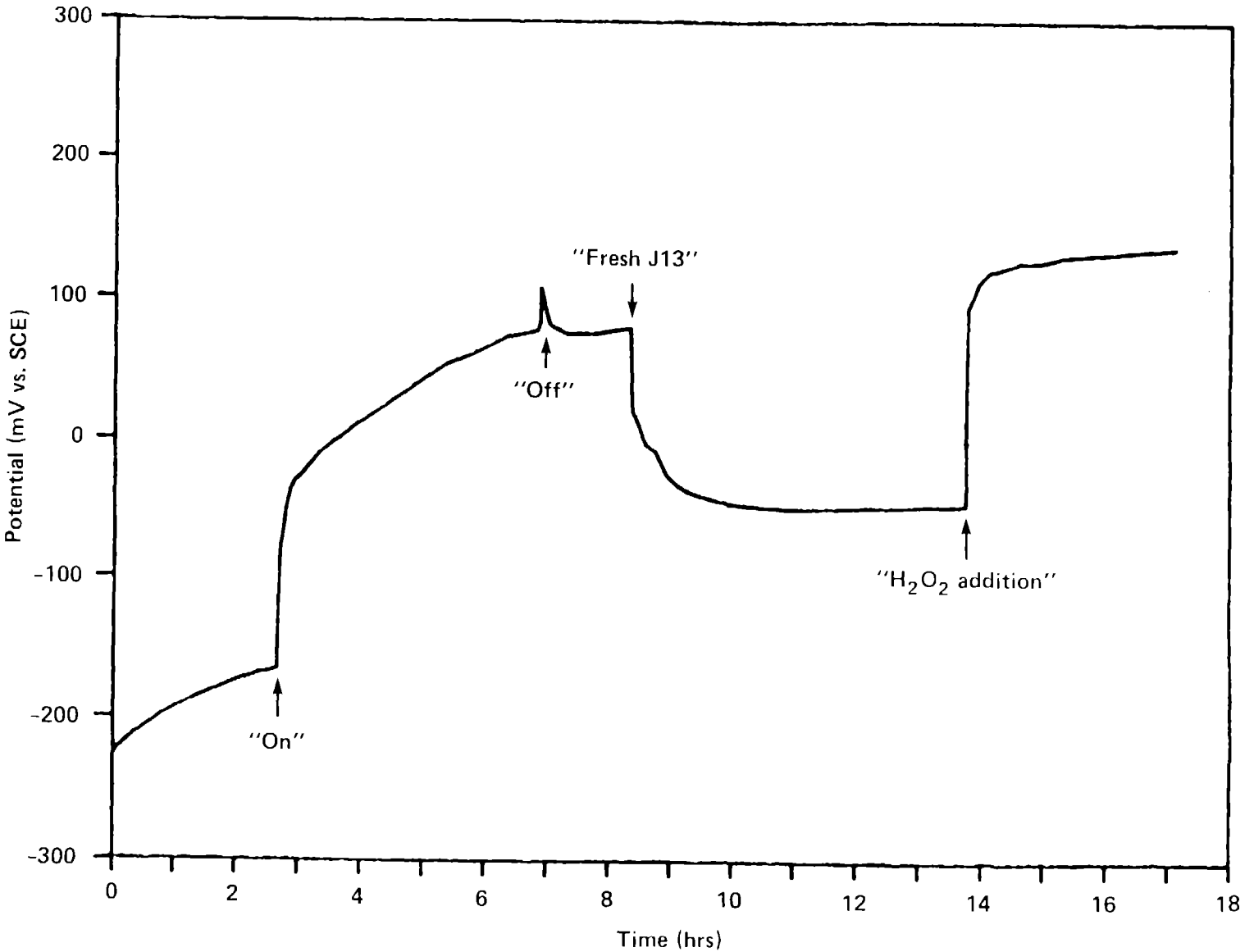
300
200
100
0
-100
-200
-300
Potential (mV vs. SCE)
"Fresh J13"
"Off"
"On"
"H_2O_2 addition"
0
2
4
6
8
10
12
14
16
18
Time (hrs)

FIGURE 3

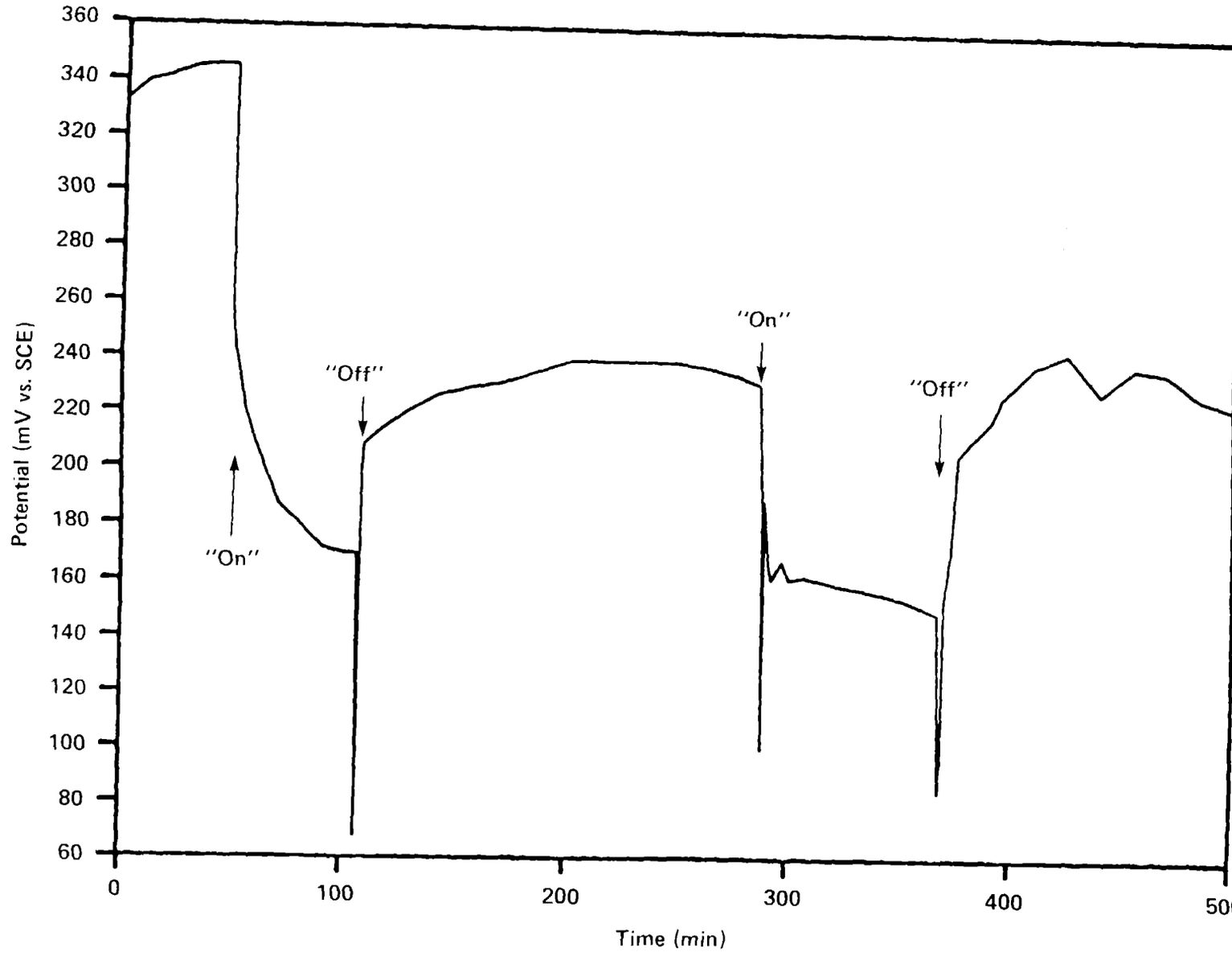
360
340
320
300
280
260
240
220
200
180
160
140
120
100
80
60
Potential (mV vs. SCE)
"On"
"Off"
"On"
"Off"
0
100
200
300
400
500
Time (min)

FIGURE 4

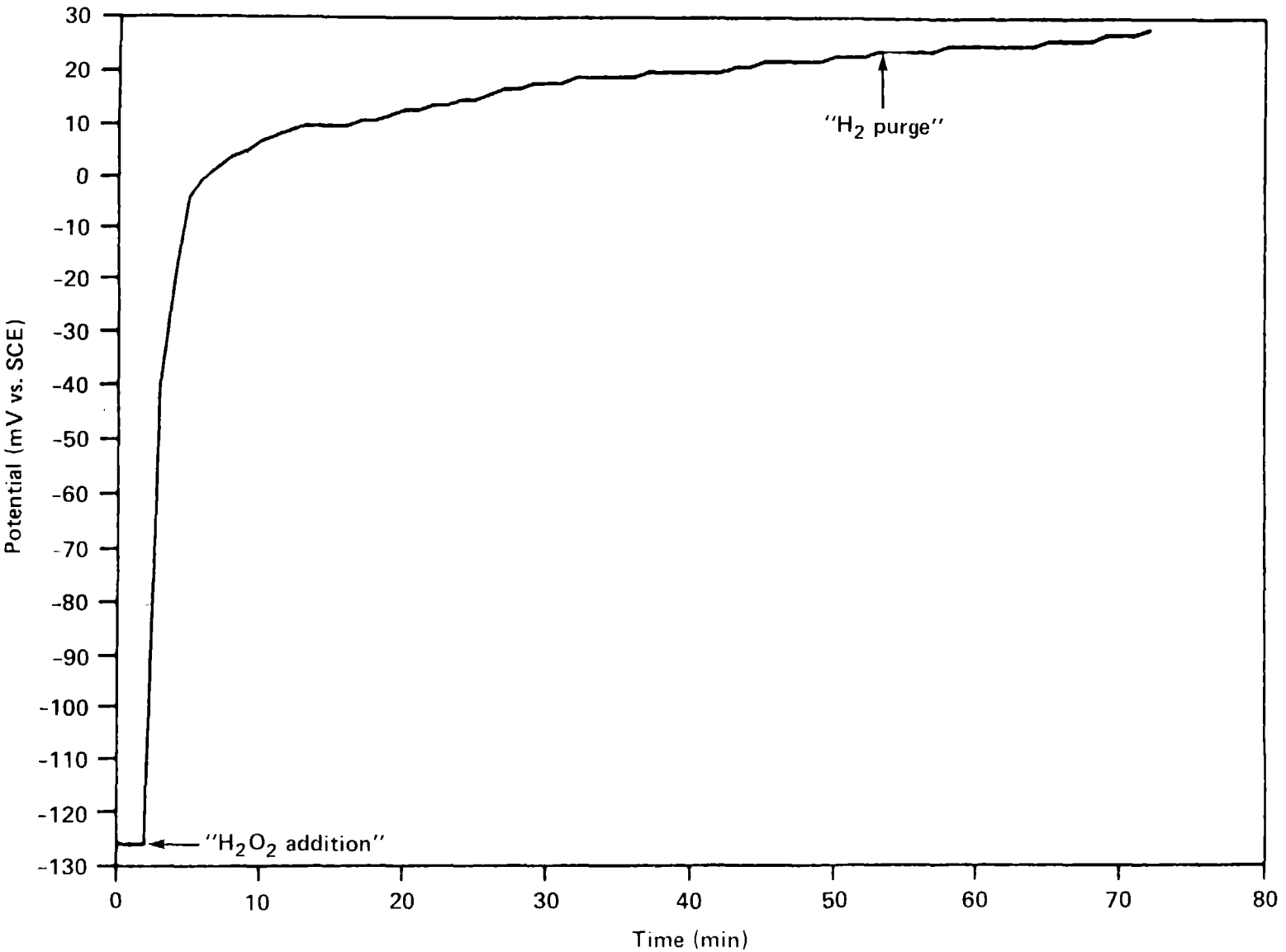
30
20
10
0
-10
-20
-30
-40
-50
-60
-70
-80
-90
-100
-110
-120
-130
Potential (mV vs. SCE)
"H2 purge"
"H2O2 addition"
0
10
20
30
40
50
60
70
80
Time (min)

FIGURE 5

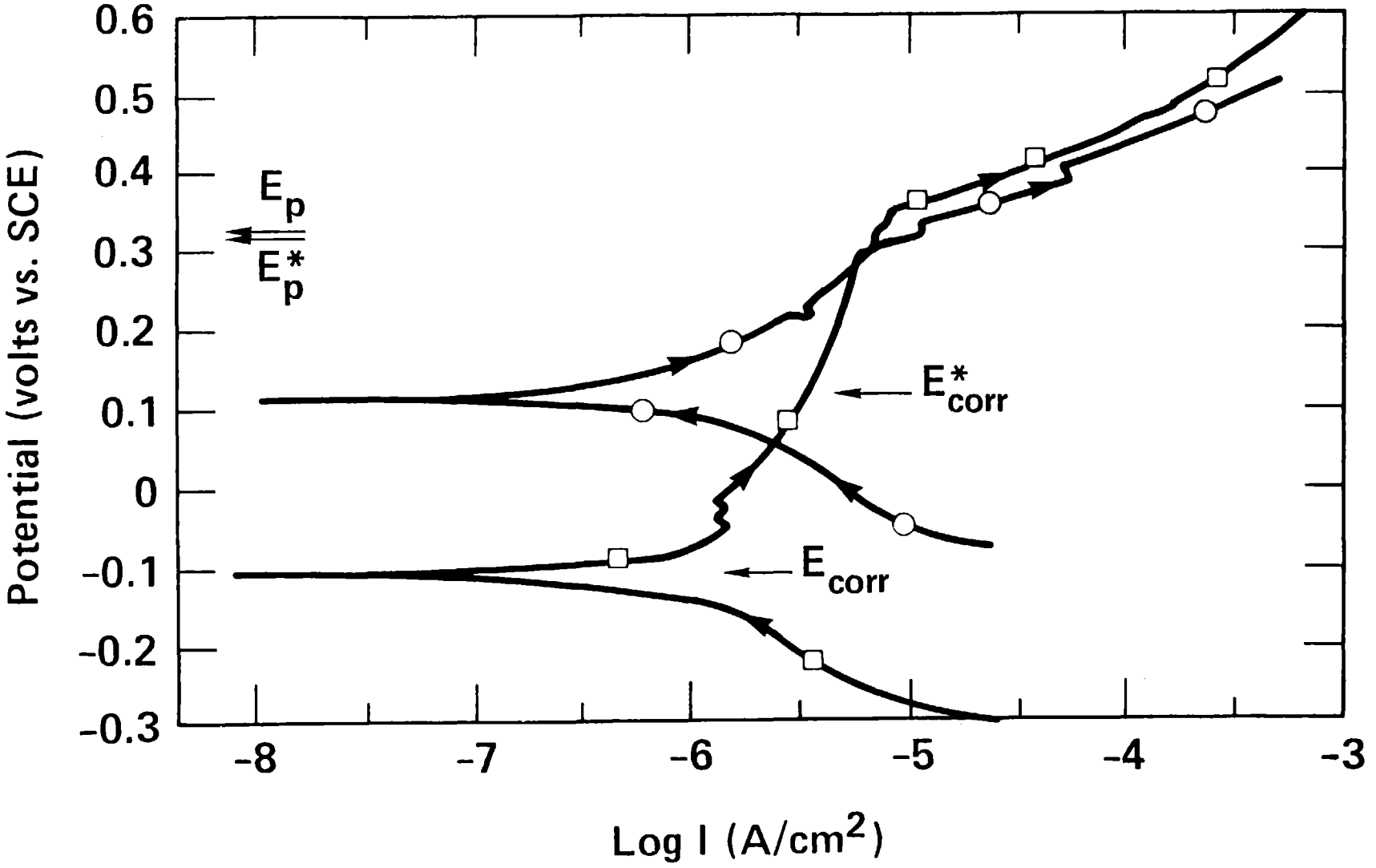
0.6
0.5
0.4
0.3
0.2
0.1
0
-0.1
-0.2
-0.3
Potential (volts vs. SCE)
E_p
E_p^*
E^*_{corr}
E_{corr}
-8
-7
-6
-5
-4
-3
Log I (A/cm^2)

FIGURE 6